

Supplementary Information

Exploration of the Interaction Strength at the Interface of Neutral Chalcogen Ligands and Gold Surfaces

Talia Alexandra Garzón¹, Monica Calatayud², Mary Tabut^{2,3}, Fernando Mendizabal^{4*}, María Luisa Cerón^{*1}

¹Facultad de Ingeniería, Universidad Finis Terrae, Av. Pedro de Valdivia 1509, Providencia, Santiago, Chile

² Sorbonne Université, CNRS, MONARIS, CNRS-UMR 8233, 4 Place Jussieu, F-75005 Paris, France

³Sorbonne Université, CNRS, Laboratoire de Chimie Théorique, LCT, 4 Place Jussieu, F-75005 Paris, France

⁴ Departamento de Química, Facultad de Ciencias, Universidad de Chile, Casilla 653, Santiago, Chile.

*Correspondence: hagua@uchile.cl (F.M.), lceron@uft.cl (M.L.C)

	Au-32 $\overline{1}$ (Clean)	SH2- Au-32 $\overline{1}$	SeH2- Au-32 $\overline{1}$
Side view			
Top view			
d(Au-Au) Å	2.776	2.761	2.768
Δd Å	0.00	0.015	0.008

Figure S1. Side and top views of the clean Au-32 $\overline{1}$ surface and the most stable adsorption geometries obtained for the XH₂ species (X = S, Se). The lower panel reports the average Au–Au distance in the surface layer together with the relaxation Δd relative to the clean slab. Adsorption induces only minimal structural distortion ($\Delta d \leq 0.02$ Å), indicating that the stepped morphology of Au321 is largely preserved.

	Au-110 (Clean)	TeH ₂ -Au110	TeHCH ₃ -Au110
Side view			
Top view			
$d_{\text{Au-Au}}$ (Å)	2.830	2.859	2.873
Δd (Å)	0.00	0.029	0.043

Figure S2. Side and top views of the clean Au(110) surface and the most stable adsorption geometries obtained for TeH₂ and TeHCH₃. The lower panel summarizes the average surface Au–Au distances and the corresponding relaxation Δd relative to the clean slab. Adsorption of Te-containing species leads to somewhat larger distortions than those observed for S- and Se-containing adsorbates, with $\Delta d \approx 0.03\text{--}0.05$ Å, while the characteristic row-like morphology of Au(110) remains essentially unchanged.

	Au-321 (Clean)	SHCH ₃ -Au321	SeHCH ₃ -Au321
Side view			
Top view			
$d_{\text{Au-Au}} (\text{\AA})$	2.775	2.723	2.718
Δd (\text{\AA})	0.00	0.052	0.057

Figure S3. Side and top views of the clean Au(321) surface and the most stable adsorption geometries obtained for the XHCH₃ species (X = S, Se). The lower panel reports the average Au–Au distance in the topmost layer and the relaxation Δd relative to the clean slab. Adsorption at step-edge Au atoms produces moderate but localized distortions ($\Delta d \approx 0.05 \text{ \AA}$), consistent with the higher reactivity of high-index stepped facets.

	SHC ₆ H ₁₁ -Au-321	SeC ₆ H ₁₁ -Au321	TeC ₆ H ₁₁ -Au321
Side view			
Top view			
d _{Au-Au} (Å)	2.736	2.729	2.733
Δd (Å)	0.039	0.046	0.042

Figure S4. Side and top views of the most stable adsorption geometries of the XC₆H₁₁ species (X = S, Se, Te) on the Au(321) surface. The lower panel displays the average Au–Au distance in the surface layer and the corresponding relaxation Δd relative to the clean slab. The bulkier C₆H₁₁ substituent enhances surface relaxation slightly ($\Delta d \approx 0.04\text{--}0.05$ Å), though the stepped topology of Au(321) is maintained.

Table S1. Comparison between the total energies and adsorption energies obtained using the r²SCAN meta-GGA functional (with and without rVV10 dispersion correction) and those

calculated in this work using the GGA+D3 approach (IVDW=11). Two representative systems

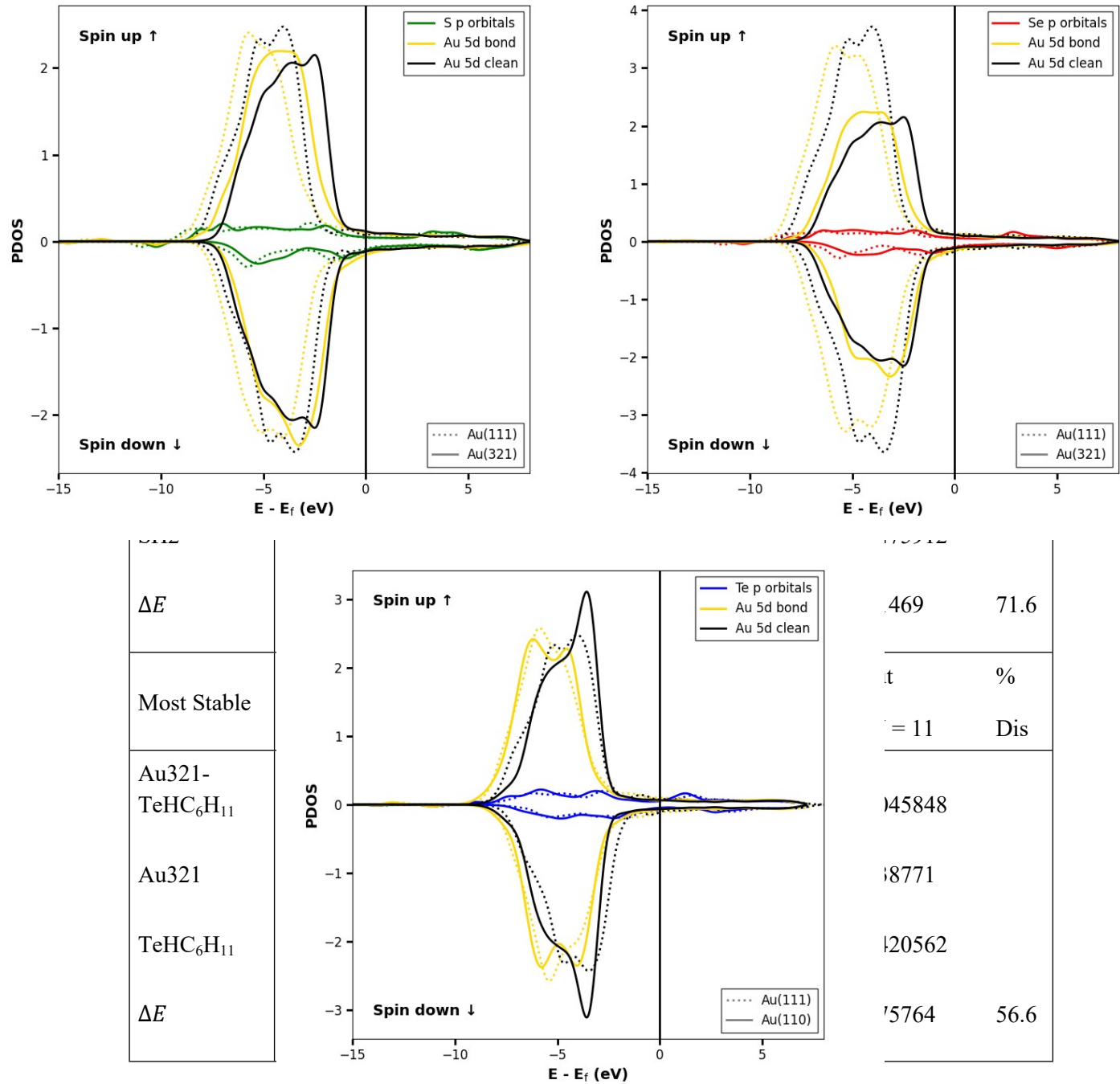


Figure S5: Spin-polarized projected density of states (PDOS) for systems AuXHCH_3 with chalcogen ($\text{X} = \text{S, Se, Te}$) p-orbitals and gold 5d-orbitals on clean and adsorbed surfaces.

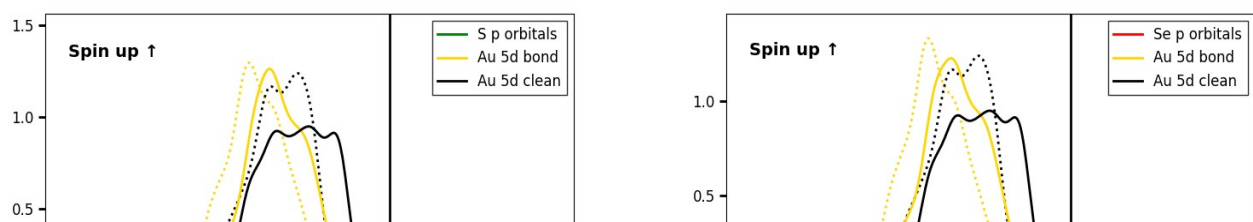


Figure S6: Spin-polarized projected density of states (PDOS) for systems $\text{AuXHC}_6\text{H}_{11}$ with chalcogen ($\text{X} = \text{S, Se, Te}$) p-orbitals and gold 5d-orbitals on clean and adsorbed surfaces.